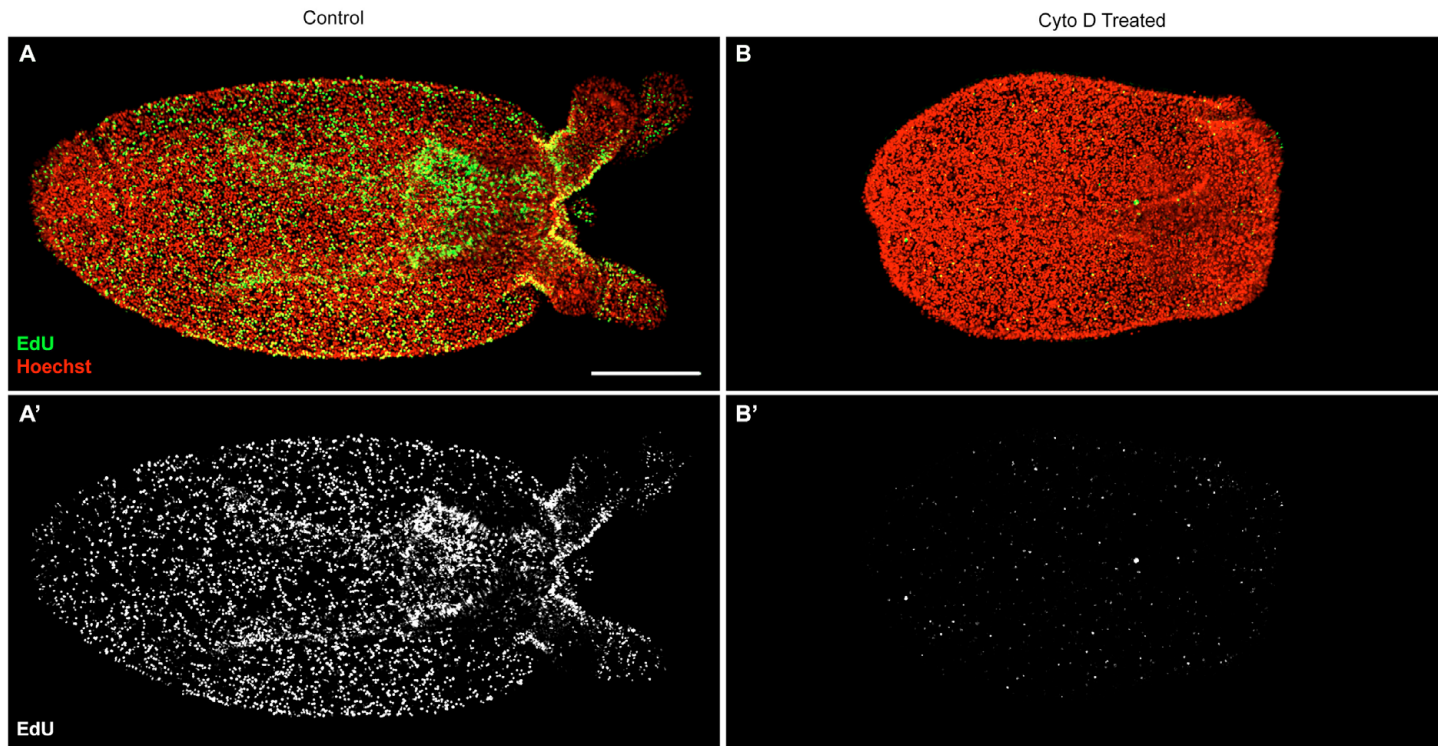
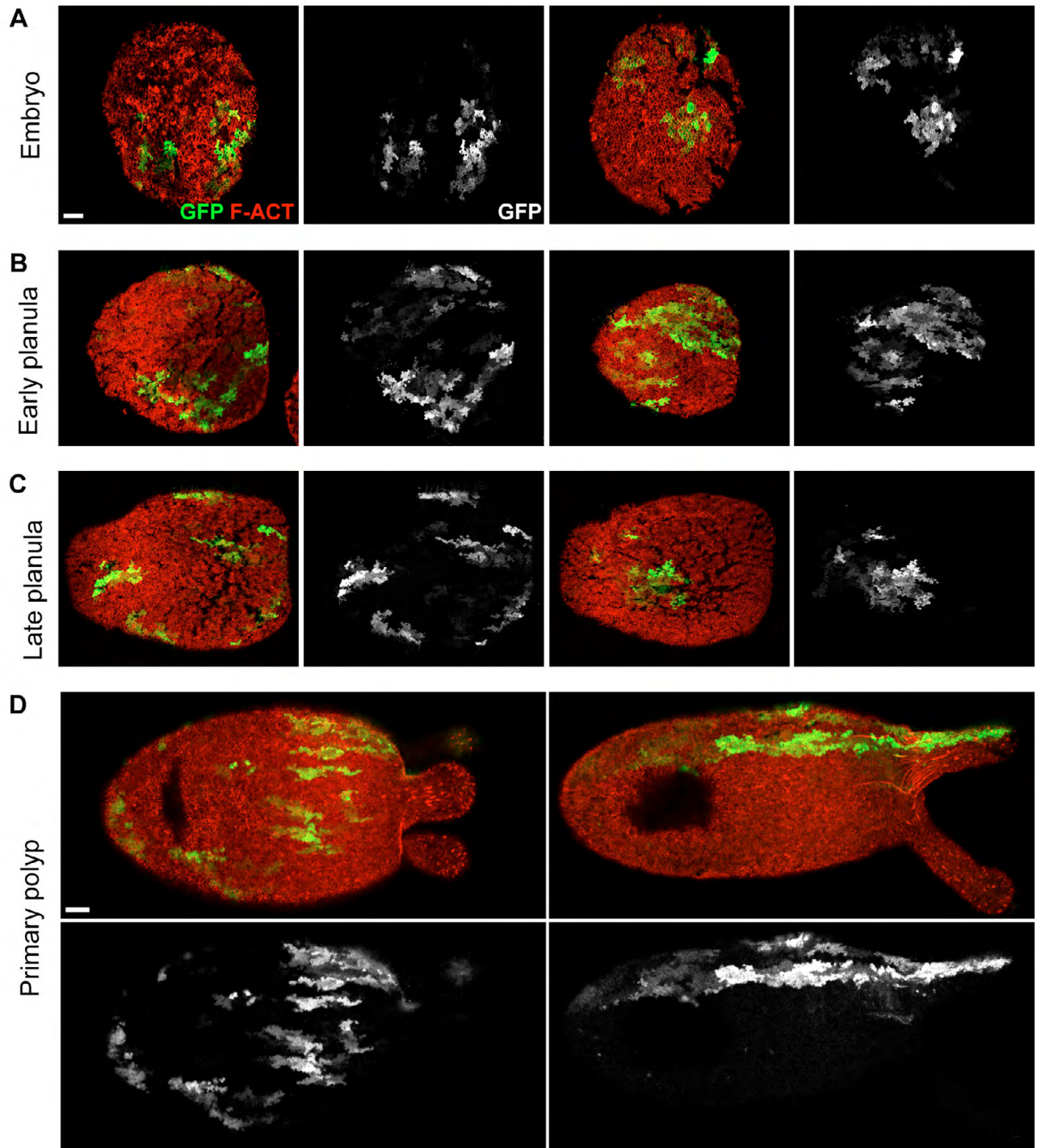


**Fig. S1. Cell shape changes in the endoderm during development.** (A-D) Animals at subsequent stages of development were stained with phalloidin to label F-Actin (green) and Hoechst to label nuclei (red). As the body column ectoderm progressively obtains a flattened morphology, the endoderm appears to make a similar transition. Brackets indicate the approximate thickness of the endodermal cell layer. Scale bar: 10  $\mu$ m.



**Fig. S2. Cell proliferation is reduced with Cyto D treatment.** Control (A,A') and Cyto D-treated (B,B') animals were stained for EdU incorporation (green) and nuclei (Hoechst; red). Although Cyto D-treated animals still show some proliferation (B'), it is reduced compared with controls (A'). Scale bar: 100  $\mu$ m.



**Fig. S3. Additional examples of Ubiquitin-GFP-injected animals showing the shape of ectodermal GFP-marked cell clusters during body column and tentacle elongation.** GFP-marked cell clones (green) in animals stained with phalloidin to label F-Actin (red), showing additional examples of clone shape in embryos (**A**) and early planula larvae (**B**). Elongating cell clones appear in late planula larvae (**C**). Primary polyps exhibit highly elongated clones along the oral-aboral axis (**D**). Scale bars: 25  $\mu$ m.



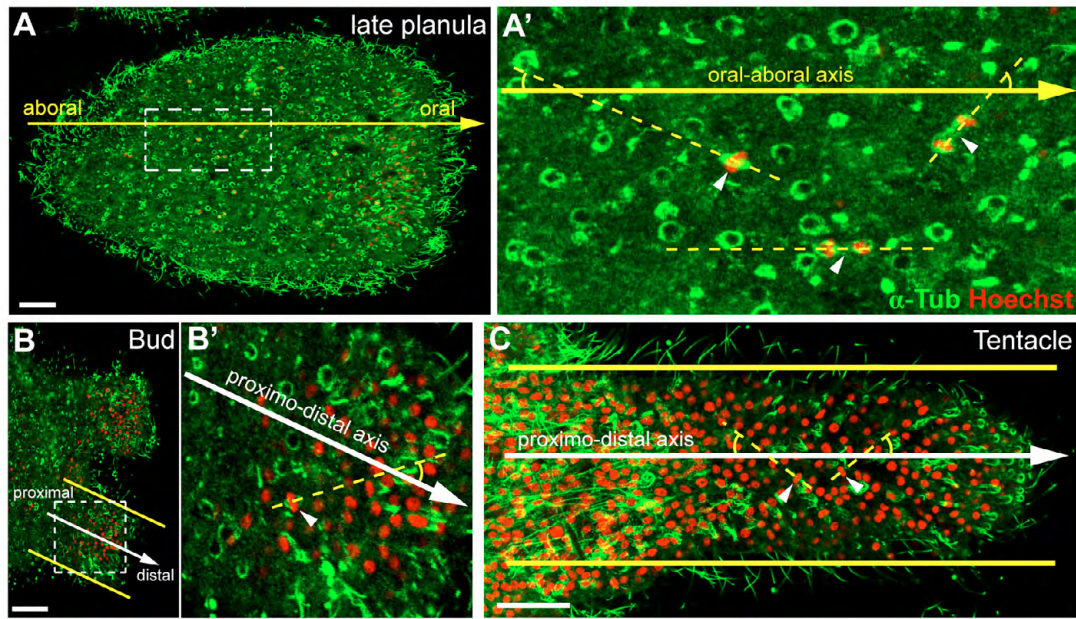


**Fig. S4. Method for measurement of the orientation of cell division.** (A,A') During body column elongation, the angle between the mitotic spindle (dashed yellow line) and the oral-aboral axis (solid yellow arrow) was defined as the spindle angle. White arrowheads indicate mitotic figures. (B-C) In both developing buds (B,B') and tentacles (C), the angle of the spindle was measured from the proximodistal axis (solid white arrow). This axis is parallel to the thickness of the bud and tentacle (solid yellow lines). Scale bars: 25  $\mu\text{m}$ .

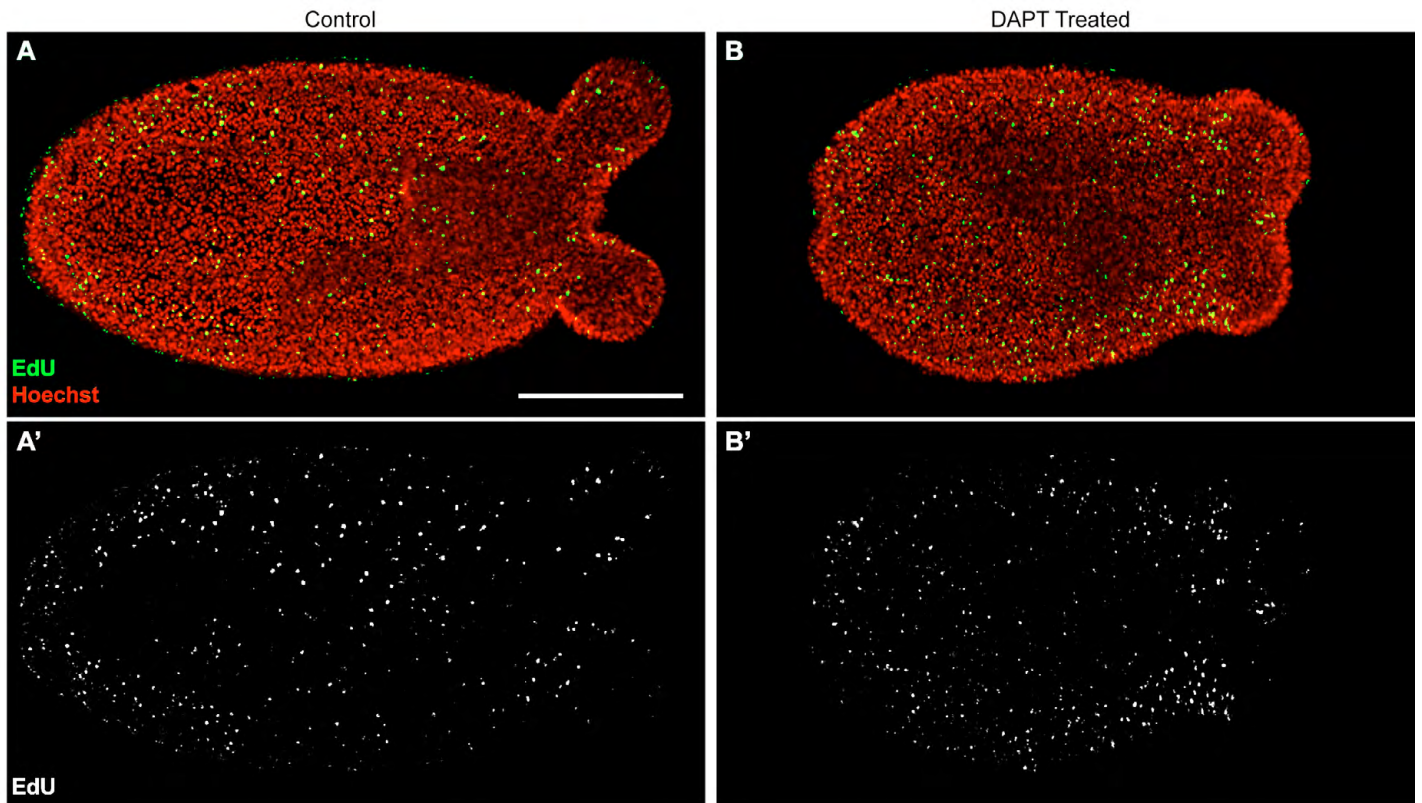


**Fig. S5. Cell proliferation is not affected by inhibition of Notch signaling.** (A,B) Confocal stacks of animals stained for EdU incorporation (green) and nuclei (Hoechst; red) for control (A) and DAPT-treated (B) animals. (A',B') EdU channel from A,B. DAPT-treated animals still had many EdU-positive cells (B'). Scale bar: 100  $\mu\text{m}$ .

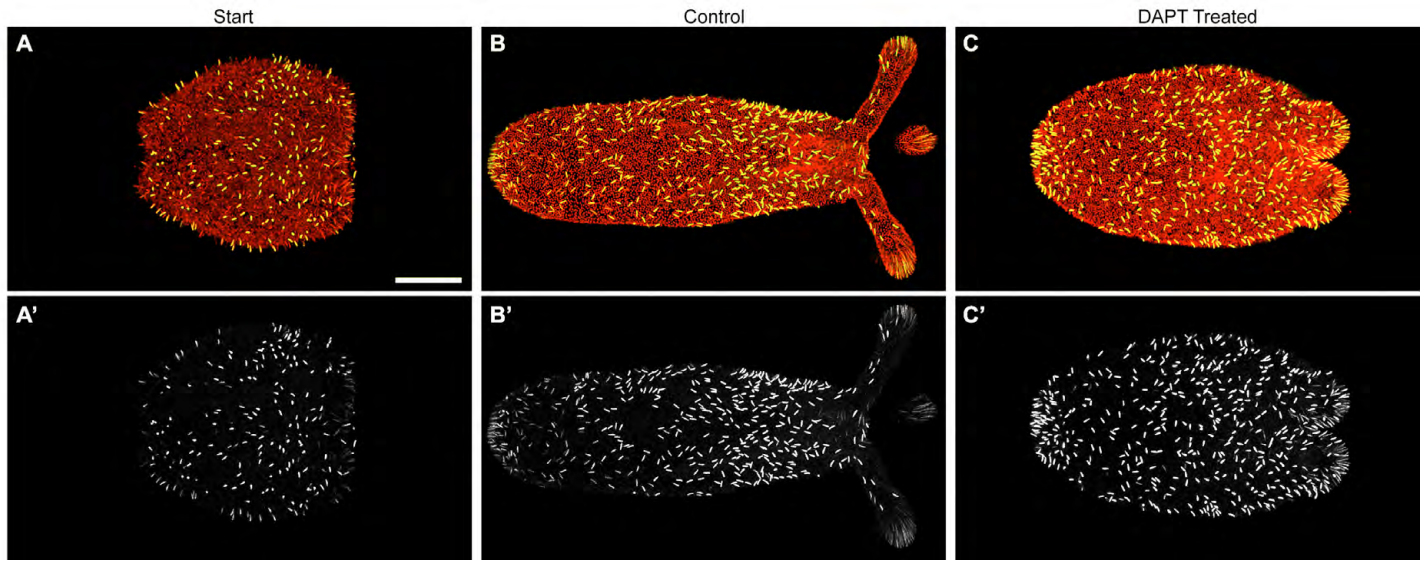


**Fig. S6. Inhibition of Notch signaling during elongation did not dramatically alter cnidocyte localization.** Confocal stacks of animals stained with DAPI to visualize cnidocytes. Animals at the start of the experiment (A,A') had cnidocytes. Both control (B,B') and DAPT-treated (C,C') animals had many cnidocytes all over their bodies. Red channel shows nuclei and cnidocytes excited by the UV laser. The green channel and bottom row (A'-C') show cnidocytes excited by the 488 laser. Scale bar: 100  $\mu$ m.

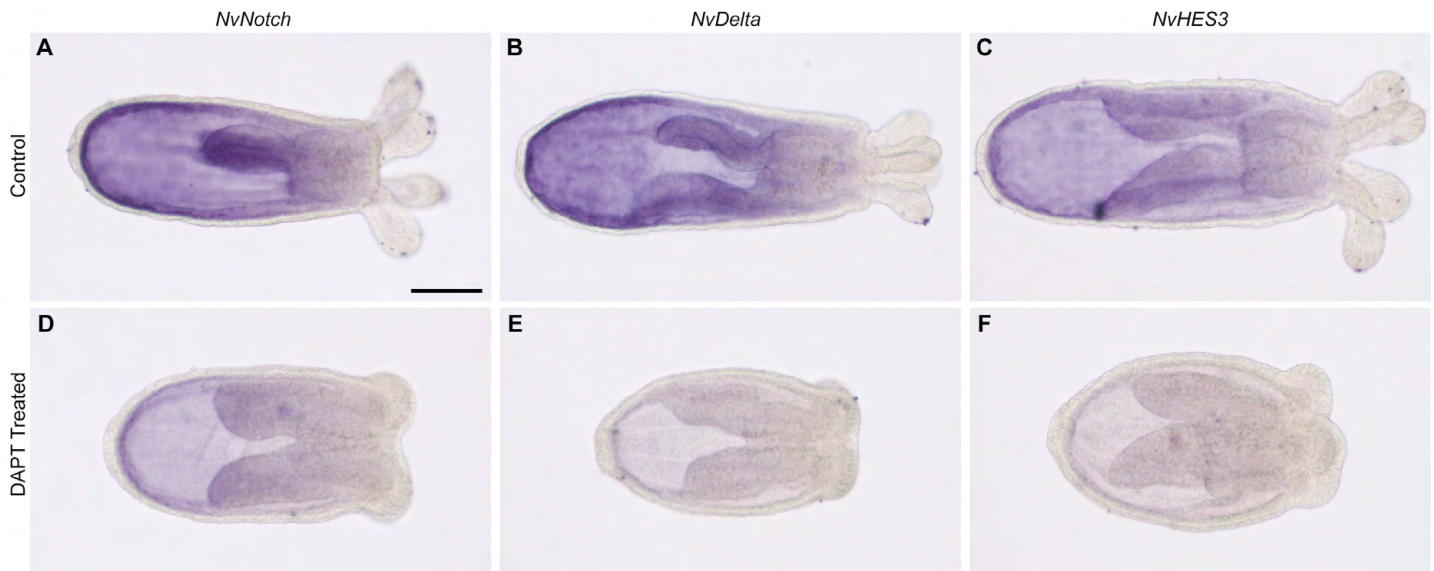


**Fig. S7. Notch pathway components have unchanged expression patterns after DAPT treatment.** (A-C) RNA *in situ* expression patterns of *NvNotch* (A), *NvDelta* (B) and *NvHES3* (C) in control animals. Expression of these transcripts was endodermal. (D-F) Corresponding expression patterns in DAPT-treated animals. All of the Notch pathway components had similar expression patterns in control and DAPT-treated animals. The DAPT-treated animals may downregulate all of these genes, as observed by reduced *in situ* staining. Scale bar: 100  $\mu$ m.



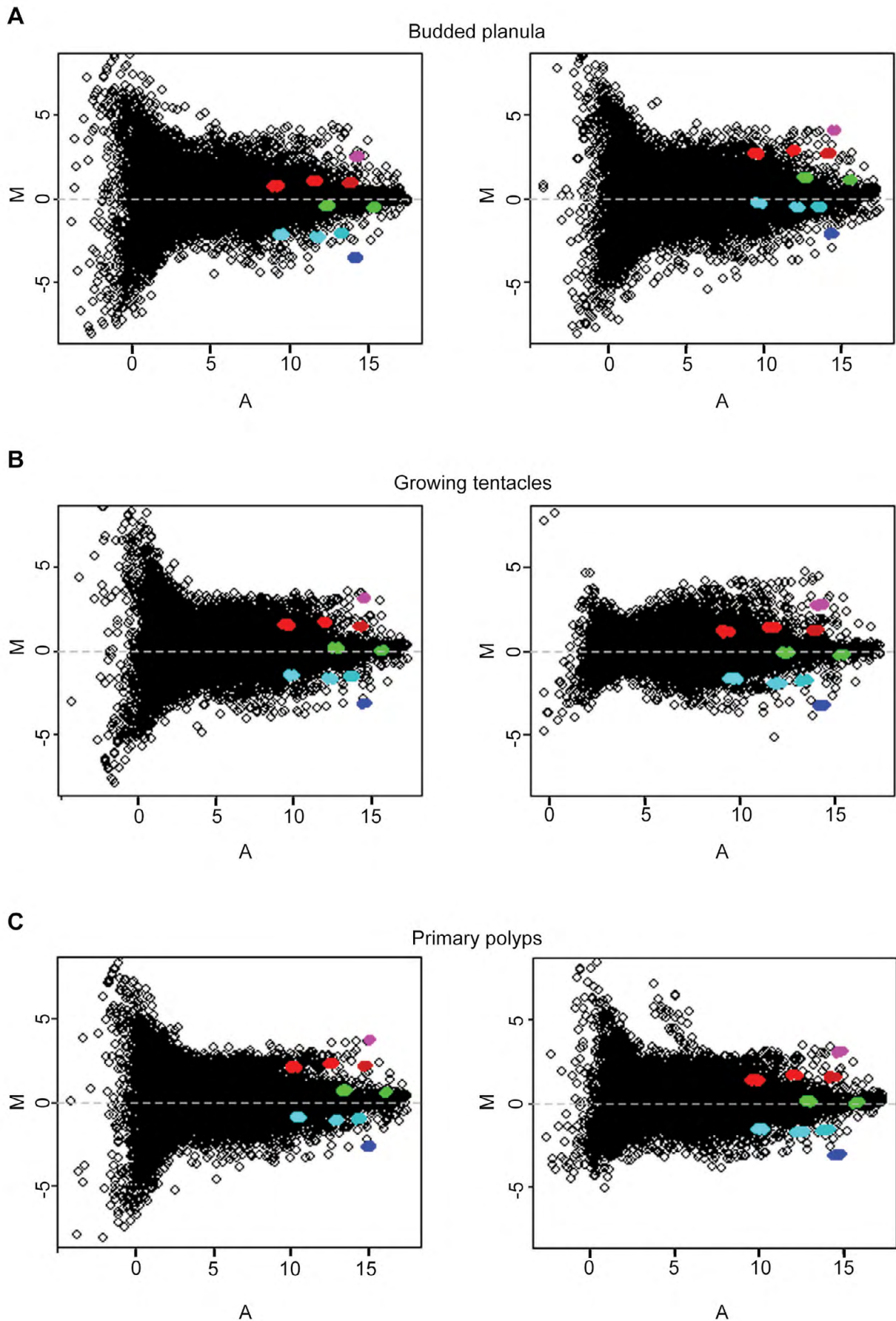


**Fig. S8. Duplicate microarray analyses show high correlation and reproducibility.** MA plots of normalized duplicate microarray analyses from budded planula (**A**), animals with growing tentacles (**B**) and primary polyps (**C**). Colored dots represent spots on the microarray. Duplicate experiments demonstrated consistent results.

**Table S1. Genes screened by *in situ* hybridization after DAPT treatment**

Sequence	Accession	Expression pattern change?
ZicC	AB231868	No
OtxA	FJ824849	No
OtxB	FJ824850	Yes
OtxC	FJ824851	No
Crossveinless-2	XM_001625111	No
Homeobrain	HM004558	No
Anthox2	AF085283.1	No
FoxL2	JGI: 82873608	No
Forkhead1	XM_001630267.1	No
Forkhead2	XM_001638841.1	No
Growth factor receptor	XM_001637818	No
G protein receptor	XM_001636348.1	No

**Table S2. Tentacle domain markers identified in the microarray screen**

Sequence	Accession	Primer pair for <i>in situ</i> probe
Anthox2	AF085283.1	CATGTCTTCGTCCTTCTACATTGACT AGGTTGCCCGAATATAGTACATT
FoxL2	JGI: 82873608	ATTAAGTGTGTCACACACAAGCGC TTCATGTACGGGTATACAGGAGGTAC
Forkhead1	XM_001630267.1	CACCGCACCCTGCAGCAAT CCTGCGACGGAAATCCCCT
Forkhead2	XM_001638841.1	GGATGATGCAAAGCAAGCGA TCTCAGAGGGATGTTTAGCCGA
Growth factor receptor-like	XM_001637818	CTTGCACTCATTGACCGACATG ACGATTGGATTGCGTGGTTG
G protein receptor-like	XM_001636348.1	ATGTCCACAAACACAAGCACCTC AGAAAATCTTGTCGGCGGTCT

**Table S3. *In situ* hybridization primer pairs**

Sequence	Accession	Primer pair for <i>in situ</i> probe
OtxB	FJ824850	AAGAGCTGGGGGCCACGGATTACATC TATCTCGGCGCCATGGAATGCACG
Notch	JN982705	GCATGGGCTTTGCTTGGATT CAGTTACTCCCAGTGTATCCAGGTCT
Delta	JN982706	ATGCAGCTACTACCACTCCAGCCA GACACGCGCCATCAAAGCAA
HES3	JN982709	GGCCGTTGACTGCATCGATA TGTGCTGACGATAGTCGTCTGC